

# Impacts of radiation exposure on the bacterial and fungal microbiome of small mammals in the Chernobyl Exclusion Zone

Rachael E. Antwis<sup>1</sup>  | Nicholas A. Beresford<sup>1,2</sup>  | Joseph A. Jackson<sup>1</sup>  |  
 Ross Fawkes<sup>1</sup> | Catherine L. Barnett<sup>2</sup> | Elaine Potter<sup>2</sup> | Lee Walker<sup>2</sup> |  
 Serge Gaschak<sup>3</sup> | Michael D. Wood<sup>1</sup> 

<sup>1</sup>School of Science, Engineering and Environment, University of Salford, Salford, UK

<sup>2</sup>UK Centre for Ecology & Hydrology, Lancaster Environment Centre, Bailrigg, UK

<sup>3</sup>Chernobyl Center for Nuclear Safety, Radioactive Waste and Radioecology, International Radioecology Laboratory, Slavutych, Ukraine

## Correspondence

Rachael E. Antwis

Email: r.e.antwis@salford.ac.uk

## Funding information

Natural Environment Research Council

Handling Editor: Fleur Ponton

## Abstract

1. Environmental impacts of the 1986 Chernobyl Nuclear Power Plant accident are much debated, but the effects of radiation on host microbiomes have received little attention to date.
2. We present the first analysis of small mammal gut microbiomes from the Chernobyl Exclusion Zone in relation to total absorbed dose rate, including both caecum and faeces samples.
3. We provide novel evidence that host species determines fungal community composition, and that associations between microbiome (both bacterial and fungal) communities and radiation exposure vary between host species. Using ambient versus total weighted absorbed dose rates in analyses produced different results, with the latter more robust for interpreting microbiome changes at the individual level. We found considerable variation between results for faecal and gut samples of bank voles, suggesting faecal samples are not an accurate indicator of gut composition.
4. Associations between radiation exposure and microbiome composition of gut samples were not robust against geographical variation, although we identified families of bacteria (Lachnospiraceae and Muribaculaceae) and fungi (Steccheriaceae and Strophariaceae) in the guts of bank voles that may serve as biomarkers of radiation exposure.
5. Further studies considering a range of small mammal species are needed to establish the robustness of these potential biomarkers.

## KEYWORDS

<sup>90</sup>Sr, <sup>137</sup>Cs, amplicon sequencing, dissymmetry, mouse, Red Forest, vole

## 1 | INTRODUCTION

Multicellular organisms host a complex community of microbes (the microbiome) that is critical for host health and function (McFall-Ngai et al., 2013; Mckenny et al., 2018). The gut microbiota has been

shown to affect animal development, immune response, food digestion and behaviour (Viney, 2019). The microbiome composition of wild mammals varies according to biological and environmental factors such as host species (e.g. Knowles et al., 2019), host age (e.g. McKenny et al., 2015; Weldon et al., 2015), diet (e.g. Maurice

This is an open access article under the terms of the Creative Commons Attribution License, which permits use, distribution and reproduction in any medium, provided the original work is properly cited.

© 2021 The Authors. *Journal of Animal Ecology* published by John Wiley & Sons Ltd on behalf of British Ecological Society

et al., 2015; McKenney et al., 2018), season (e.g. Maurice et al., 2015) and contaminant-induced stress (e.g. Zhang et al., 2020), among others (Antwis et al., 2020). Less well-understood is the relationship between radiation exposure and microbiome composition, particularly in wild animal systems.

Over the last decade, there has been a growing interest in the effect of contaminants on the composition of the gut microbiome, with some studies reporting changes in the two most prevalent bacterial phyla within the gut, namely Firmicutes and Bacteroidetes (Jin et al., 2017; Weldon et al., 2015; Wu et al., 2016). Different chemical stressors have been found to affect Firmicute: Bacteroidete (F:B) ratios, with As (Lu et al., 2014), Cd (Zhang et al., 2015), chlorpyrifos (Joly Condetto et al., 2015), permethrin (Nasuti et al., 2016) and pentachlorophenol (Kan et al., 2015) leading to decreases in F:B, whereas Pb (Wu et al., 2016) and carbendazim (Jin et al., 2015) exposure increases F:B ratios. Environmental pollutants can impact the gut microbiota resulting in changes to metabolite production and the immune system (reviewed in Jin et al., 2017). For example, colonic inflammation in mice has been shown to be associated with reduced F:B in the gut microbiota following pesticide exposure (Jin et al., 2016). Similarly, in rats, silver nanoparticle exposure decreases Firmicute abundance in the gut, with associated disturbance of immunomodulatory gene expression in the ileum (Williams et al., 2015). Consequently, pollutant exposure may increase the susceptibility of animals to some diseases.

High acute radiation exposure (>1 Gy) influences the gut microbial communities (e.g. Dubois & Walker, 1988; Packey & Ciorba, 2011). The administration of bacterial probiotics (particularly *Lactobacillus* spp.) can compensate for this in both humans and model organisms, reducing radiation-induced diarrhoea (Demers et al., 2014; Goudarzi et al., 2016; Liu et al., 2017; A. Zhang & Steen, 2018). These responses of the gut microbiome to high acute radiation doses have led to the suggestion that the gut microbiota could be a potential biomarker of radiation exposure (Goudarzi et al., 2016; Zhang & Steen, 2018).

At lower radiation exposures in contaminated environments, such as the Chernobyl Exclusion Zone (CEZ), some studies report changes in particular taxa of the animal microbiome (Lavrinenko, Mappes, et al., 2018; Lavrinenko et al., 2018). For example, Lavrinenko, Mappes, et al. (2018) report a reduction in F:B of faecal samples from bank voles *Myodes glareolus* at their most contaminated sites (mean ambient dose rate 30  $\mu$ Sv/hr), and radiation-induced changes in the bacterial communities of feathers have been suggested for birds in the Chernobyl region (Czirják et al., 2010; Ruiz-González et al., 2016). Conversely, Lavrinenko, Tukalenko, et al. (2018) found no effect of radiation on the skin microbiome of bank voles. If consistent relationships between microbiome and chronic low-level (and environmentally relevant) radiation exposure can be identified, this would present a valuable biomarker for evaluating radiological exposure internationally.

The extent to which radiation exposure is affecting wildlife in Chernobyl is highly contested (Beresford et al., 2020; Mousseau & Moller, 2011). A fundamental problem with many of the studies undertaken to date is that they use ambient dose rates (often reported

in units of absorbed radiation dose rate for humans,  $\mu$ Sv/hr), rather than estimating the total absorbed dose rate of study organisms, accounting for both internal and external exposure (Beaugelin-Seiller et al., 2020). As such, it has not been possible to accurately determine dose–effect relationships, making interpretation of these studies difficult. Here we present the first study of gastrointestinal (GI) tract microbiome composition in CEZ small mammals for which individual total absorbed dose rates have been estimated. Previous studies in the CEZ have only considered the bacterial microbiome of one small mammal species (bank vole) using faecal samples; here we report on the faecal microbiome of four small mammal species using faecal samples, as well as the first direct analysis of the gut microbiome using caecum samples from bank voles. In addition, our microbiome analysis includes both bacteria and fungi, extending the limited general knowledge on the fungal component of animal microbiomes.

## 2 | MATERIALS AND METHODS

### 2.1 | Field sampling in the Red Forest (2017)

The study was undertaken in line with ethical approval obtained from the University of Salford. In August 2017, we sampled small mammals from the Red Forest, an area of c. 4–6 km<sup>2</sup> over which pine trees were killed by radiation in 1986; subsequently, there has been sparse regrowth of deciduous trees and some understorey vegetation. In 2016, approximately 80% of the Red Forest was damaged by fire (Beresford et al., 2021). Our 2017 sampling sites (Figure 1) included a total of eight sites across three burn categories, namely 'burnt with regrowth' ( $n = 2$ ), 'burnt with minimal regrowth' ( $n = 3$ ) and 'unburnt' ( $n = 3$ ). At each of these sampling sites, a 60 m  $\times$  60 m trapping grid was used, with traps positioned at 10-m intervals (each grid comprised a total of 49 traps). To maximise trapping success, the trapping grids were established 1 week prior to the beginning of the study and pre-baited with rolled oats and carrots/cucumber. Trapping occurred over 8 consecutive days; traps were baited and set each evening and visited early in the morning to retrieve captured small mammals. The small mammals were transferred to the Chernobyl field station where each animal was live-monitored to determine its <sup>137</sup>Cs whole-body activity concentration using an unshielded 51 mm  $\times$  51 mm NaI (TI) detector (GMS 310 core gamma logger) supplied by John Caunt Scientific Ltd. Additional regular background measurements were made each day. The detector was calibrated using the results for small mammals ( $n = 14$ ) that were live-monitored with the GMS 310 and subsequently analysed using a calibrated detector at the Chernobyl Center's main laboratory ( $R^2 = 0.98$ ). The limit of detection (LOD) was estimated as three times the standard deviation of the background measurement. The sex of each animal was determined and their live mass recorded.

Freshly excreted faecal samples were collected (in the laboratory) directly from animals for subsequent microbiome analysis. We sampled striped field mice *Apodemus agrarius* ( $n = 29$ ), yellow-necked mice *Apodemus flavicollis* ( $n = 58$ ), wood mice *Apodemus sylvaticus*

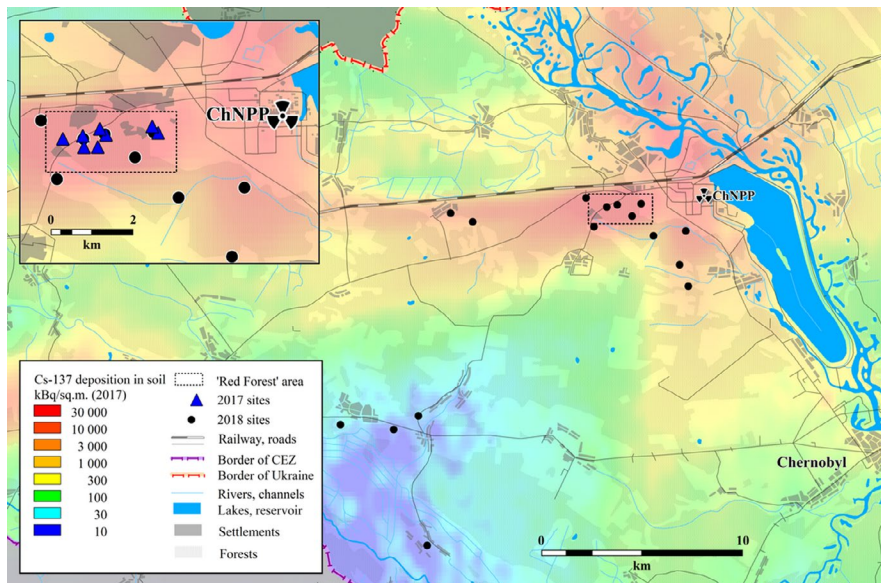


**FIGURE 1** Location of the study sites in the CEZ where small mammals were trapped in 2017 and 2018; the approximate location of the Red Forest is indicated by the black rectangle. The underlying  $^{137}\text{Cs}$  soil data shown (decay corrected to summer 2017) are from the study by Shestopalov (1996)

( $n = 27$ ) and bank voles *Myodes glareolus* ( $n = 22$ ; Table 1). Faecal samples were immediately placed into vials containing 100% ethanol and subsequently stored at  $-20^{\circ}\text{C}$ . Samples were transported under licence to the University of Salford (UK); sample integrity was maintained during transit using dry ice, and the samples were then stored at  $-20^{\circ}\text{C}$  prior to DNA extraction. We used fur clipping to mark each small mammal prior to release at the point of capture, ensuring each collection over subsequent days was from a new animal. Only faeces from new animal captures were included in this study.

## 2.2 | Field sampling across the CEZ (2018)

Small mammals were trapped in July/August 2018 over 10 consecutive days, with only bank voles included in this study. Twelve transects of Sherman traps were established at sites across a gradient of ambient dose rates (Figure 1). Each transect measured 290 m with a trap interval of 10 m (30 traps per transect). The 2018 sampling used the same protocol for baiting and collection of animals as in 2017. For some of the analyses, bank voles from 2018 have been categorised by collection 'site category', defined as inside or outside the Red Forest (all of the 2018 sites inside the Red Forest were burnt to some degree by the 2016 fire; Table 1).

Captured animals were transferred to the Chernobyl field station, where each animal was live-monitored to quantify the whole-body activity concentrations of both  $^{137}\text{Cs}$  and  $^{90}\text{Sr}$  using a new field portable Radioanalysis of Small Samples (ROSS) detector developed at the University of Salford (Fawkes, 2018). ROSS comprises a holding chamber with a capacity of  $170 \times 60 \times 50$  mm. Two CsI gamma detectors (each measuring  $70 \times 40 \times 25$  mm) were mounted on opposite sides of the sample holding chamber and two plastic scintillator beta detectors were mounted, one above ( $100 \times 50 \times 0.5$  mm) and one below ( $100 \times 60 \times 0.5$  mm) the chamber. The entire assembly was enclosed within a lead shield ( $>10$  mm thickness). ROSS was

calibrated using  $^{137}\text{Cs}$  and  $^{90}\text{Sr}$  standards developed by Chernobyl Center; standards ranged from 4 to 20 g to represent small mammals. We included  $^{137}\text{Cs}$ -only standards,  $^{90}\text{Sr}$ -only standards and mixed ( $^{137}\text{Cs}$  and  $^{90}\text{Sr}$ ) standards. Counting of the  $^{137}\text{Cs}$  standards on the beta detectors provided a correction for the influence of  $^{137}\text{Cs}$  emissions on  $^{90}\text{Sr}$  recordings. Multiple background counts were performed daily (at least nine per day), and the LOD was estimated using the method described by Currie (1968).

After live-monitoring of radiation, bank voles were killed by an overdose of anaesthetic (isoflurane) followed by exsanguination (in accordance with Schedule 1 of the Animals (Scientific Procedures) Act 1986). The sex and mass of each animal was recorded. Gastrointestinal tracts ( $n = 142$ ) were dissected immediately under sterile conditions, with surfaces and instruments sterilised between each dissection. Gastrointestinal tracts were stored in laboratory vials containing 100% ethanol at  $-20^{\circ}\text{C}$ . The frozen vials were transported to the University of Salford under licence and stored as described for faeces.

## 2.3 | Dosimetry: Ambient dose rate

All dose data are provided as Supporting Information. At every trapping location in 2017 and 2018, ambient dose rate ( $\mu\text{Sv/hr}$ ) was measured using an MKS-01R metre at 5 cm above the soil surface.

## 2.4 | Dosimetry: Estimation of small mammal total absorbed dose rate for the 2017 study

Soil samples (0–10 cm soil depth) were available from each of the trapping sites used in the 2017 study. These samples were analysed using laboratory detectors at Chernobyl Centre to determine  $^{137}\text{Cs}$  and  $^{90}\text{Sr}$  activity concentrations within the soil (see Beresford,

**TABLE 1** Sample sizes of host species used in the study, and associated sex, total absorbed dose rate, burn and site categories for these samples. Animals estimated to receive total absorbed dose rates of  $<4 \mu\text{Gy/hr}$  were assigned 'low', those with estimated dose rates of  $4\text{--}42 \mu\text{Gy/hr}$  assigned 'medium', and those  $>42 \mu\text{Gy/hr}$  assigned to the 'high' category. All samples from 2017 were collected within the Red Forest but from areas that had experienced different degrees of damage from forest fires. Samples from 2018 were either collected within or outside the Red Forest

Year	Sample type	Host species	Sex		Total absorbed dose category						Burn category			Site category	
			Total n	Female	Male	Unidentified	Low	Medium	High	Burnt (regrowth)	Burnt (minimal regrowth)	Unburnt	Inside Red Forest	Outside Red Forest	
2017	Faeces	Bank vole	22	5	16	1	0	0	22	3	1	18	All	—	
2017	Faeces	Striped field mouse	29	10	18	1	0	7	22	15	0	14	All	—	
2017	Faeces	Wood mouse	27	6	20	1	0	0	27	2	25	0	All	—	
2017	Faeces	Yellow-necked mouse	58	28	29	1	0	7	51	19	17	22	All	—	
2018	Gut (caecum)	Bank vole	132	54	78	0	42	64	26	—	—	—	26	106	

Barnett, et al., 2020 for methodology). For each small mammal species, an external dose conversion coefficient was calculated using the ERICA Tool version 1.2 (Brown et al., 2016). To define the geometry for each species, the length, width and height were determined through literature review. Soil activity concentrations were inputted into the ERICA Tool, and external dose rates were estimated using the derived external dose conversion coefficients and appropriate occupancy factors (assuming 50% of time in soil and 50% on the soil surface for mice and 70% in soil and 30% on soil for bank voles).

The measured  $^{137}\text{Cs}$  whole-body activity concentrations were used to determine the internal absorbed dose from  $^{137}\text{Cs}$ . In 2017, the internal  $^{90}\text{Sr}$  activity concentrations were not directly measured; these were estimated using the species-specific transfer parameters measured in the CEZ (Beresford, Barnett, et al., 2020) and the soil  $^{90}\text{Sr}$  activity concentrations for the appropriate sampling site. For each small mammal species, an internal dose conversion coefficient was calculated using the ERICA Tool and the same assumed geometries as used for the external dose conversion coefficient derivation. The ERICA Tool was then run using the default radiation weighting factors to calculate the total weighted absorbed dose rate. While other radionuclides (e.g. Pu-isotopes and  $^{241}\text{Am}$ ) are present in the CEZ, Beresford, Barnett, et al. (2020) demonstrated that the contribution of these isotopes to the total absorbed dose rate of small mammals within the Red Forest was low ( $<10\%$ ).

For each individual animal, the total weighted absorbed dose rate (hereafter referred to as the total absorbed dose rate) was calculated by summing the internal and external dose rates for that individual.

## 2.5 | Dosimetry: Estimation of small mammal total absorbed dose rate for the 2018 study

Soil activity concentrations were not available for all of the sites within the 2018 study. However, Beresford, Barnett, et al. (2020) and Beresford et al. (2008) demonstrated that, at worst, the estimated external dose from  $^{137}\text{Cs}$  and the external ambient dose field at sites in the CEZ differ by a factor of 3. Based on our small mammal dose rate data from 2017, the mean ratio of external dose from  $^{137}\text{Cs}$  to the external ambient dose field is 0.98. Therefore, the external gamma dose rates measured at each trapping location were used to estimate the external absorbed dose rate for each small mammal using the occupancy factors defined above. Note the ERICA Tool assumes a shielding effect from fur and skin for external beta exposure (Ulanovsky et al., 2008); this assumption was also adopted by the International Commission on Radiological Protection (ICRP, 2008). The estimated contribution of  $^{90}\text{Sr}$  (a beta emitter) to the external whole-body dose rate of small mammals is therefore negligible and could be ignored for the 2018 study.

The  $^{137}\text{Cs}$  and  $^{90}\text{Sr}$  whole-body activity concentrations measured using ROSS were input into the ERICA Tool, and the species-specific internal dose conversion coefficients were used to estimate the

internal absorbed dose rate for each animal. At the lowest contamination sites in 2018, some of the whole-body activity concentrations for both  $^{137}\text{Cs}$  and  $^{90}\text{Sr}$  were below the LOD. Using these LOD values to determine total absorbed internal dose rate led to a maximum estimated dose of 0.6  $\mu\text{Gy/hr}$ , introducing some uncertainty in radiation exposure estimates at the lowest end of our total absorbed dose rate range.

## 2.6 | Dosimetry: Incorporation of estimated dose rates with subsequent analyses

The ICRP has, over the last decade, developed an approach to radiological protection of the environment based on the concept of Reference Animals and Plants (RAPs; ICRP, 2008). Defined at the family level, the RAPs represent key organisms that are likely to be present within locations requiring radiological assessment. The ICRP has suggested Derived Consideration Reference Levels (DCRLs) for these RAPs, which are the order of magnitude dose rate bands within which radiation-induced effects that could impact on the population may be expected (ICRP, 2008). We assigned animals to total absorbed dose rate categories based on the suggested DCRL for ICRP Reference Rat (ICRP, 2008), that is, approximately 4–42  $\mu\text{Gy/hr}$ . As such, animals estimated to receive total absorbed dose rates of <4  $\mu\text{Gy/hr}$  (i.e. below the dose rate at which effects would be anticipated for mammals) were assigned 'low'. Those with estimated dose rates of 4–42  $\mu\text{Gy/hr}$  (i.e. within the band of anticipated effects) were assigned 'medium', and those >42  $\mu\text{Gy/hr}$  (i.e. above the dose rate at which effects would be anticipated for mammals) were assigned 'high'. The 'high' and 'low' total absorbed dose rates are in effect also a comparison of inside and outside the Red Forest due to the high radionuclide deposition that occurred in the area now known as the "Red Forest" (i.e. the 'inside' and 'outside' Red Forest site categories; Table 1).

We correlated ambient and total estimated absorbed dose rates using a Spearman's rank correlation. To quantify whether correlation coefficients varied based on the radiation dose measure used, we also repeated the correlations for each total absorbed dose rate category separately and visualised these using a scatterplot in ggplot2 (Wickham, 2009).

## 2.7 | DNA extraction and molecular work

For faecal samples, we extracted DNA from the full sample (~0.1 g) of the four host species. For gut samples, we isolated ~25% of the distal end of the caecum of bank voles and homogenised the contents by hand in sterile Petri dishes, before weighing out ~0.1 g for DNA extraction. We conducted all DNA extractions using the PureLink™ Microbiome DNA Purification Kit (Invitrogen) according to the manufacturer's instructions.

To identify bacterial communities, we conducted 16S rRNA gene amplicon sequencing of the v4 region using F515 and R806 primers

(~250 bp; Caporaso et al., 2010, according to Kozich et al., 2013; Griffiths et al., 2018). Briefly, we ran PCRs in duplicate using Solis BioDyne 5x HOT FIREPol® Blend Master Mix, 2  $\mu\text{M}$  primers and 15 ng of sample DNA under thermocycling conditions of 95°C for 10 min; 25 cycles of 95°C for 30 s, 55°C for 20 s and 72°C for 30 s; and a final extension of 72°C for 8 min. We included negative (extraction blanks) and positive (mock community) controls. We combined PCR replicates into a single PCR plate and cleaned these using HighPrep™ PCR clean up beads (MagBio) according to the manufacturers' instructions. We quality checked PCR products throughout on an Agilent 2200 TapeStation. To quantify the number of sequencing reads per sample, we constructed a library pool using 1  $\mu\text{l}$  of each sample and conducted a titration sequencing run using this pool with a v2 nano cartridge (2 × 150 bp) on the Illumina MiSeq platform. We calculated the volume of each sample required based on the percentage of reads obtained per sample and pooled these accordingly. We sequenced the final normalised library using paired-end (2 × 250 bp) reads on a v2 cartridge on an Illumina MiSeq at the University of Salford.

We identified fungal communities by sequencing the ITS gene using ITS1F and ITS2 primers (~150–500 bp) using a modified protocol of Smith and Peay (2014) and Nguyen et al. (2015), as in Griffiths et al. (2019). We ran PCRs in duplicate using thermocycling conditions of 95°C for 10 min, followed by 28 cycles of 95°C for 30 s, 54°C for 45 s and 72°C for 60 s; with a final extension at 72°C for 10 min. We included extraction blanks and a mock community as negative and positive controls respectively. We quantified and normalised individual libraries as described above, before conducting full paired-end sequencing using Illumina v2 (2 × 250 bp) chemistry on an Illumina MiSeq at the University of Salford.

## 2.8 | Pre-processing of amplicon sequencing data

We conducted all data processing and analysis in RStudio (v1.2.1335; RStudio Team, 2016) for R (v3.6.0; R Core Team, 2017). A total of 13,371,018 raw sequence reads were generated during 16S rRNA gene amplicon sequencing, which we processed in DADA2 v1.5.0 (Callahan et al., 2016). Modal contig length was 253 bp once paired-end reads were merged. We removed sequence variants (SVs) with length >260 bp (26 SVs; 0.002% of total sequences) along with chimeras and five contaminant SVs identified using the DECONTAM package (Davis et al., 2017). We assigned taxonomy using the SILVA v132 database (Quast et al., 2013; Yilmaz et al., 2014). DADA2 identified 20 unique SVs in the sequenced mock community sample comprising 20 bacterial isolates. We stripped out mitochondria from samples along with SVs with <0.0001% abundance across all samples. We removed three samples from which poor sequence data were obtained (<1,000 reads), leaving a median of 28,563 reads (7,101 to 132,106) per sample. We exported the final SV table, taxonomy table and sample metadata to the PHYLOSEQ package (McMurdie & Holmes, 2013).

We obtained a total of 2,778,887 raw sequence reads during ITS gene sequencing. We trimmed the remaining adapters and primers using cutadapt (Martin, 2011) in RStudio. As with 16S rRNA sequence data, we pre-processed ITS amplicons in DADA2 v1.5.0 (Callahan et al., 2016). Modal contig length was 219 bp (167–457 bp) once paired-end reads were merged. We did not conduct additional trimming based on sequence length as the ITS region is highly variable (Schoch et al., 2012). We removed chimeras and one contaminant using the DECONTAM package, and then assigned taxonomy using the UNITE v7.2 database (UNITE, 2017). DADA2 identified 12 unique SVs in the sequenced mock community sample comprising 12 fungal isolates. We removed 54 samples from which poor sequence data were obtained (<500 reads), leaving a median of 1875 reads (506 to 17,226) per sample. As with 16S rRNA data, we exported the final SV table, taxonomy table and sample metadata to the PHYLOSEQ package (McMurdie & Holmes, 2013) for subsequent analysis.

## 2.9 | Community analyses

For both bacterial and fungal community data, we normalised the clean count data using centred-log ratio (clr) transformations (Gloor et al., 2017) in phyloseq (McMurdie & Holmes, 2013), and visualised beta-diversity (based on species and sample types, i.e. gut or faeces) using PCA plots with Euclidean distances in ggplot2 (Wickham, 2009). We used PERMANOVAs to test for differences in beta-diversity according to species, sample type, sex and total absorbed dose rate category using the adonis function in the VEGAN package, performing marginal tests for individual terms (Oksanen et al., 2018). We agglomerated the data to family level and visualised differences in clr-transformed data according to the five sampling groups (faecal samples from the three mice species, plus faecal and gut samples from bank voles) using jitter box plots in ggplot2 (Wickham, 2009). We tested for differences between sampling groups in the clr-transformed values of these 24 families (12 per microbial kingdom) using Kruskal–Wallis nonparametric tests with Dunn's pairwise tests and Hochberg-adjusted *p* values in the dunn.test and FSA packages (Dinno, 2017; Ogle et al., 2019). We also converted the raw SV counts to relative abundance and visualised the 12 most abundant families (for each kingdom separately) as a stacked chart according to species and sample type.

We then split the clr-transformed data by sampling year and reran the PERMANOVA for the 2017 faecal samples based on species, sex, total absorbed dose rate category, grid line and burn category using marginal tests. We visualised the variation in clr-transformed values for the 12 most abundant genera in faecal samples from yellow-necked mice (as this was the only species with sufficient samples across all three burn categories; Table 1) using PCA plots of beta-diversity and jitter plots for the clr values of the 12 most abundant genera. We also reran the PERMANOVA with marginal tests for the 2018 gut data with total absorbed dose rate category, site category,

sex and transect line as predictor variables, and again visualised these using PCA plots of beta-diversity and jitter plots of the clr values of the 12 most abundant genera for each microbial kingdom separately. Additionally, we looked for stochastic effects of radiation on the microbiome using the betadisper function in the VEGAN package to test for variation in the dispersion (i.e. the variation around the mean) of the bank vole gut data according to radiation category.

To determine whether microbiome beta-diversity correlated with total absorbed dose rate independent of geographic location, we conducted partial Mantel tests using the VEGAN package (Oksanen et al., 2018) on (a) the gut samples from bank voles and (b) across faecal samples from the four mammal species. For each sample type, we constructed between-sample distance matrices in phyloseq (McMurdie & Holmes, 2013) for bacteria and fungi separately using Euclidean distances of clr-transformed data. We then generated Euclidean distance matrices from the total absorbed dose rate data for each individual using the PROXY package (Meyer & Buchta, 2019). Finally, we constructed a geographic distance matrix between radiation distance and samples using longitude and latitude coordinates in Microsoft Excel. We then ran partial Mantel tests with Spearman's rank correlation between total absorbed dose rate distance and microbiome distance (for bacteria and fungi separately) for each sample type, with geographic distance matrices as a covariate.

For (a) bank vole gut data and (b) faecal sample data from all four small mammals, we calculated alpha-diversity (SV richness and the inverse Simpson index as a measure of community evenness) of bacterial and fungal communities by subsampling the raw SV count table to a standardised number of reads (equal to the sample with the lowest number of reads) using an iterative approach (100 times), and averaging the diversity estimates across these iterations. For bank vole gut data, we used Spearman's rank correlations to identify the relationship between total absorbed radiation dose and microbial alpha-diversity. For faecal sample data, we used GLMMs to test for the effect of total absorbed dose rate on alpha-diversity, with host species as a random factor.

We used Spearman's rank correlation (with Benjamini–Hochberg corrected *p* values and False Discovery Rate adjustment) in the associate function of the MICROBIOME package (Lahti & Shetty, 2017) to identify relationships between the two radiation dose measures (ambient and total) and clr-transformed 16S and ITS rRNA sequence data, agglomerated to genus level. These analyses were conducted separately for the gut and faecal samples, according to host species. We then visualised the resultant correlation coefficients using heat maps in ggplot2 (Wickham, 2009).

We calculated F:B ratios in vole guts using both clr-transformed data and data converted to relative abundance (as done by Lavrinienko, Mappes, et al., 2018). We also calculated F:B in faecal samples of all four mammal species using relative abundance data. We visualised these ratios according to total absorbed dose rate category using jitter plots. We tested for differences between total absorbed dose rate categories within a set of data using Kruskal–Wallis nonparametric tests, with Dunn's pairwise tests and Hochberg-adjusted *p* values where necessary.

### 3 | RESULTS

#### 3.1 | How do ambient dose rates compare to total absorbed dose rates?

Many previous studies of radiation effects in Chernobyl and other radioactively contaminated sites have used ambient dose rate as a proxy for total absorbed dose rate. Our results show a moderate positive correlation between ambient and total absorbed dose rates across all animals captured during both 2017 and 2018 ( $\rho = 0.529$ ,  $p < 0.001$ ). When data were split into the three different total absorbed dose rate categories, all relationships remained statistically significant [low ( $<4 \mu\text{Gy/hr}$ ):  $\rho = 0.898$ ,  $p < 0.001$ ; medium ( $4\text{--}42 \mu\text{Gy/hr}$ ):  $\rho = 0.879$ ,  $p < 0.001$ ; and high ( $>42 \mu\text{Gy/hr}$ ):  $\rho = 0.236$ ,  $p < 0.001$ ] however, the correlation for the 'high' dose data was weak (Figure S1). Given that the estimated total absorbed dose rate provides a better estimation than ambient dose rate of each individual's radiation exposure and microbiome analysis is at the individual level, we used total absorbed dose rates for the majority of our analyses, but for a few comparisons we have also presented the relationship with ambient dose rate to illustrate the limitations of this commonly used approach.

In this study, we used the ERICA dosimetry approach, which assumes shielding by fur and skin of beta radiation and consequently the external dose rates from  $^{90}\text{Sr}$  are estimated to be negligible. We acknowledge that estimates using different modelling approaches may lead to a higher estimated external dose rate from  $^{90}\text{Sr}$  (e.g. Gaschak et al., 2011). We have estimated the external dose

contributions using an alternative model (available from <https://wiki.ceh.ac.uk/x/9wHbBg>) which does not consider fur or skin shielding (Coppelstone et al., 2001; Vives i Batlle et al., 2007). Using this model, we find that the maximum difference in total dose rate estimate would be approximately 30%, with an average difference of about 10%. Animals were live-monitored to determine whole-body radionuclide activity concentrations and hence enable estimation of internal dose. While there is a potential for some external contamination (of skin and fur) to influence live-monitoring results, skinned carcasses and whole animal live-monitoring data from some of our previous small mammal studies in the CEZ (Beresford et al., 2008, 2016) demonstrate that surface contamination makes a negligible contribution to the whole-body activity concentration measurements obtained via live monitoring. Consequently, this is not a significant source of uncertainty for the present study.

#### 3.2 | How does microbiome beta-diversity vary according to host factors and total absorbed dose rate

A PERMANOVA demonstrated host species ( $F_{3,257} = 24.902$ ,  $R^2 = 0.224$ ,  $p = 0.001$ ; Figure 2; Figure S2), sample type ( $F_{1,257} = 2.820$ ,  $R^2 = 0.008$ ,  $p = 0.002$ ) and total absorbed dose rate category ( $F_{2,257} = 2.572$ ,  $R^2 = 0.015$ ,  $p = 0.001$ ) all predicted bacterial community beta-diversity, whereas sex did not ( $F_{1,257} = 1.194$ ,  $R^2 = 0.004$ ,  $p = 0.138$ ). Similarly, fungal community beta-diversity was weakly predicted by host species ( $F_{3,212} = 5.012$ ,  $R^2 = 0.066$ ,  $p = 0.001$ ; Figure 2; Figure S3), sample type ( $F_{1,212} = 3.390$ ,  $R^2 = 0.015$ ,

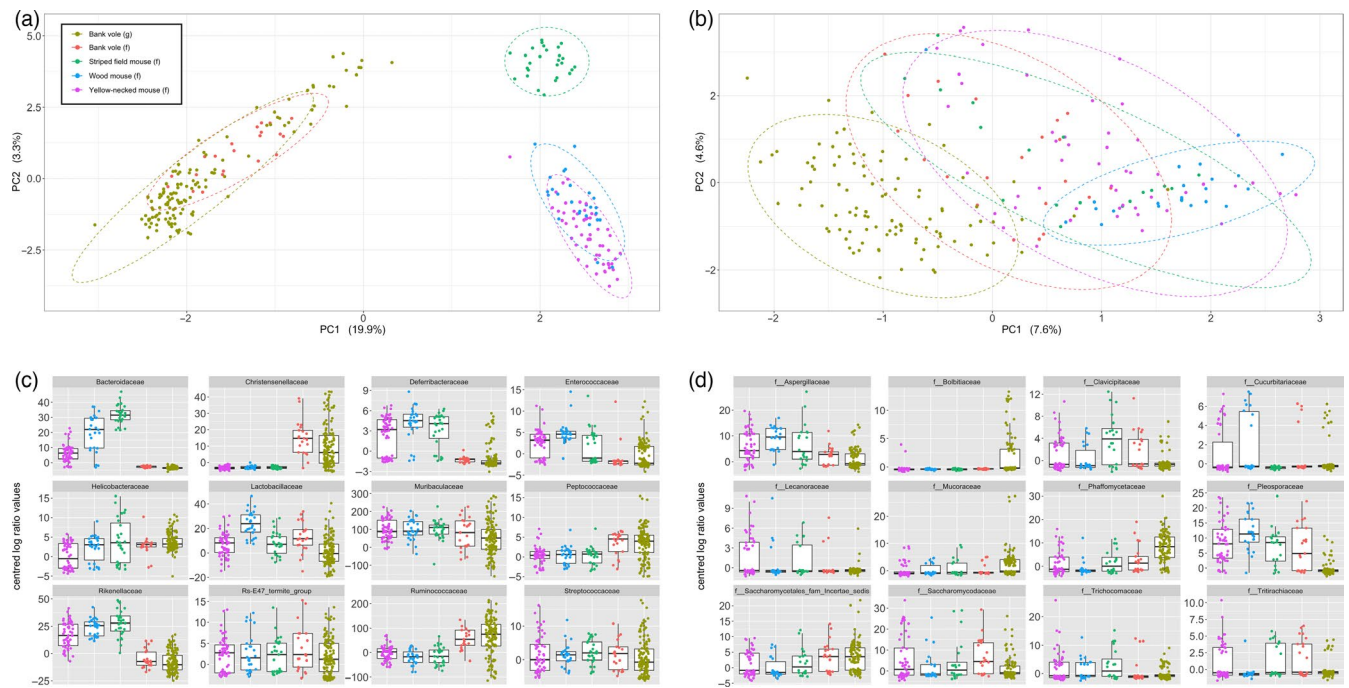


**FIGURE 2** PCA plots showing Euclidean distances of clr-transformed bacterial (a) and fungal (b) communities associated with faecal and gut samples from four small mammal species in the Chernobyl Exclusion Zone. Jitter plots displaying the clr values of the 12 most abundant bacterial (c) and fungal (d) families across the five sampling groups (faecal samples for the three mice species along with faecal and gut samples for the bank voles)

$p = 0.001$ ) and total absorbed dose rate category ( $F_{2,212} = 1.736$ ,  $R^2 = 0.015$ ,  $p = 0.001$ ), but not sex ( $F_{2,212} = 1.161$ ,  $R^2 = 0.005$ ,  $p = 0.148$ ). Differences between host species were much more evident for bacterial community composition than for fungal community composition (Figure 2a,b), for which 22.4% and 6.6% of the variation was explained by host species respectively. There were a number of differences in the clr values of the most abundant bacterial and fungal families according to host species and sample type (Figure 2c,d); a full description with statistical testing can be found in Supporting Information.

### 3.3 | How do alpha-diversity and beta-diversity of faecal samples vary according to host species, burn category and total absorbed dose rate?

When using faecal samples (i.e. 2017 data) only, the PERMANOVA indicated that host species ( $F_{3,128} = 11.944$ ,  $R^2 = 0.217$ ,  $p = 0.001$ ; Figure S4), burn category ( $F_{2,128} = 1.632$ ,  $R^2 = 0.020$ ,  $p = 0.004$ ; Figure S4) and sampling site ( $F_{5,128} = 1.562$ ,  $R^2 = 0.047$ ,  $p = 0.001$ ) had a detectable effect on beta-diversity of faecal bacterial communities, but that total absorbed dose rate category ( $F_{1,128} = 0.912$ ,  $R^2 = 0.006$ ,  $p = 0.616$ ) and sex ( $F_{1,128} = 1.103$ ,  $R^2 = 0.007$ ,  $p = 0.228$ ) did not. There were only sufficient samples for yellow-necked mice to visualise differences in microbiome composition across all three burn categories (Table 1). Although the differences were relatively small in the 12 most abundant bacterial genera, some showed directional changes based on burn category (Figure S5), for instance, *Bacteroides* were most abundant at 'burnt (minimal regrowth)' sites and least abundant at 'unburnt' sites, whereas *Ruminococcaceae*\_UCG-003 showed the inverse.

As with bacterial communities, host species ( $F_{3,111} = 1.945$ ,  $R^2 = 0.048$ ,  $p = 0.001$ ), burn category ( $F_{2,111} = 1.969$ ,  $R^2 = 0.033$ ,  $p = 0.001$ ) and site ( $F_{5,111} = 1.726$ ,  $R^2 = 0.072$ ,  $p = 0.001$ ) had a detectable effect on beta-diversity of faecal fungal communities, but total absorbed dose rate category ( $F_{1,111} = 1.157$ ,  $R^2 = 0.010$ ,  $p = 0.153$ ) and sex ( $F_{1,111} = 0.823$ ,  $R^2 = 0.007$ ,  $p = 0.911$ ) did not. Burn category effects on faecal community composition were clearer from the fungal community PCA plot (Figure S6) than for the bacterial community PCA (Figure S4); individuals captured in the burnt areas with minimal regrowth tended to appear in the lower left-hand side of the plot (Figure S6). When looking at the samples from yellow-necked mice, differences in clr values for the 12 most abundant fungal genera based on burn category were more pronounced than for bacterial genera (Figure S7). For example, yellow-necked mice sampled in unburnt areas had faecal communities characterised by low *Gelatoporia*, *Pyrenochaetopsis* and *Wickerhamomyces* relative to burnt areas, as well as high *Tritirachium* (Figure S7).

The partial Mantel test for association between microbial community beta-diversity and total absorbed dose rate distance (weighted by geographic distance) indicated there was a significant relationship for bacterial communities of faecal samples across the four host species ( $r = 0.248$ ,  $p = 0.001$ ), whereby animals that

experienced similar radiation exposure also had similar microbiome composition. However, the relationship was not statistically significant for fungal communities ( $r = -0.073$ ,  $p = 0.888$ ).

There was a significant relationship between total absorbed radiation dose and fungal community alpha-diversity across all four host species (all  $p < 0.05$ ; Table S1), whereby as radiation dose increased, fungal diversity decreased. Total absorbed radiation dose did not have a significant effect on bacterial community alpha-diversity (all  $p > 0.05$ ; Table S1).

### 3.4 | How do alpha-diversity and beta-diversity of bank vole gut samples vary according to site category and total absorbed dose rate?

The PERMANOVA showed total absorbed dose rate category ( $F_{1,128} = 3.096$ ,  $R^2 = 0.022$ ,  $p = 0.001$ ), site category (i.e. inside or outside the Red Forest;  $F_{1,128} = 2.266$ ,  $R^2 = 0.016$ ,  $p = 0.001$ ; Figure S8) and sampling site ( $F_{14,128} = 1.549$ ,  $R^2 = 0.156$ ,  $p = 0.001$ ) had a detectable effect on bacterial community beta-diversity of bank vole guts, but sex did not ( $F_{1,128} = 1.219$ ,  $R^2 = 0.009$ ,  $p = 0.056$ ). However, the actual differences in the 12 most abundant bacterial genera between vole guts inside and outside the Red Forest (i.e. site category) were relatively subtle (Figure S9). The betadisper analysis showed there were no significant differences in the dispersion of the bacterial community composition of bank vole guts based on radiation exposure category ( $F_{2,136} = 0.032$ ,  $p = 0.964$ ).

For fungal communities of bank vole gut samples, site category ( $F_{1,100} = 2.914$ ,  $R^2 = 0.027$ ,  $p = 0.001$ ), total absorbed dose rate category ( $F_{2,100} = 1.786$ ,  $R^2 = 0.017$ ,  $p = 0.001$ ; Figure S10) and sampling site ( $F_{13,100} = 1.350$ ,  $R^2 = 0.163$ ,  $p = 0.002$ ) all had a detectable effect on community beta-diversity, whereas sex did not ( $F_{1,100} = 1.266$ ,  $R^2 = 0.012$ ,  $p = 0.082$ ). Again, differences in the 12 most abundant fungal genera inside and outside the Red Forest were relatively subtle (Figure S11). As with the bacterial communities, there were no significant differences in the dispersion of the fungal community composition of bank vole guts based on radiation exposure category ( $F_{2,105} = 0.506$ ,  $p = 0.602$ ).

The partial Mantel test for association between microbial community beta-diversity and total absorbed dose rate distance (weighted by geographic distance) indicated there was no significant relationship for bacterial ( $\rho = -0.023$ ,  $p = 0.627$ ) or fungal ( $\rho = -0.047$ ,  $p = 0.740$ ) community composition of bank vole guts.

There were no significant effects of total absorbed radiation dose rate on alpha-diversity of microbial communities (all  $p > 0.05$ ; Table S2).

### 3.5 | How do different microbial taxa correlate with the two radiation dose measures?

Faecal and gut samples of bank voles showed considerably different fungal and bacterial association patterns (Figures 3 and 4; note

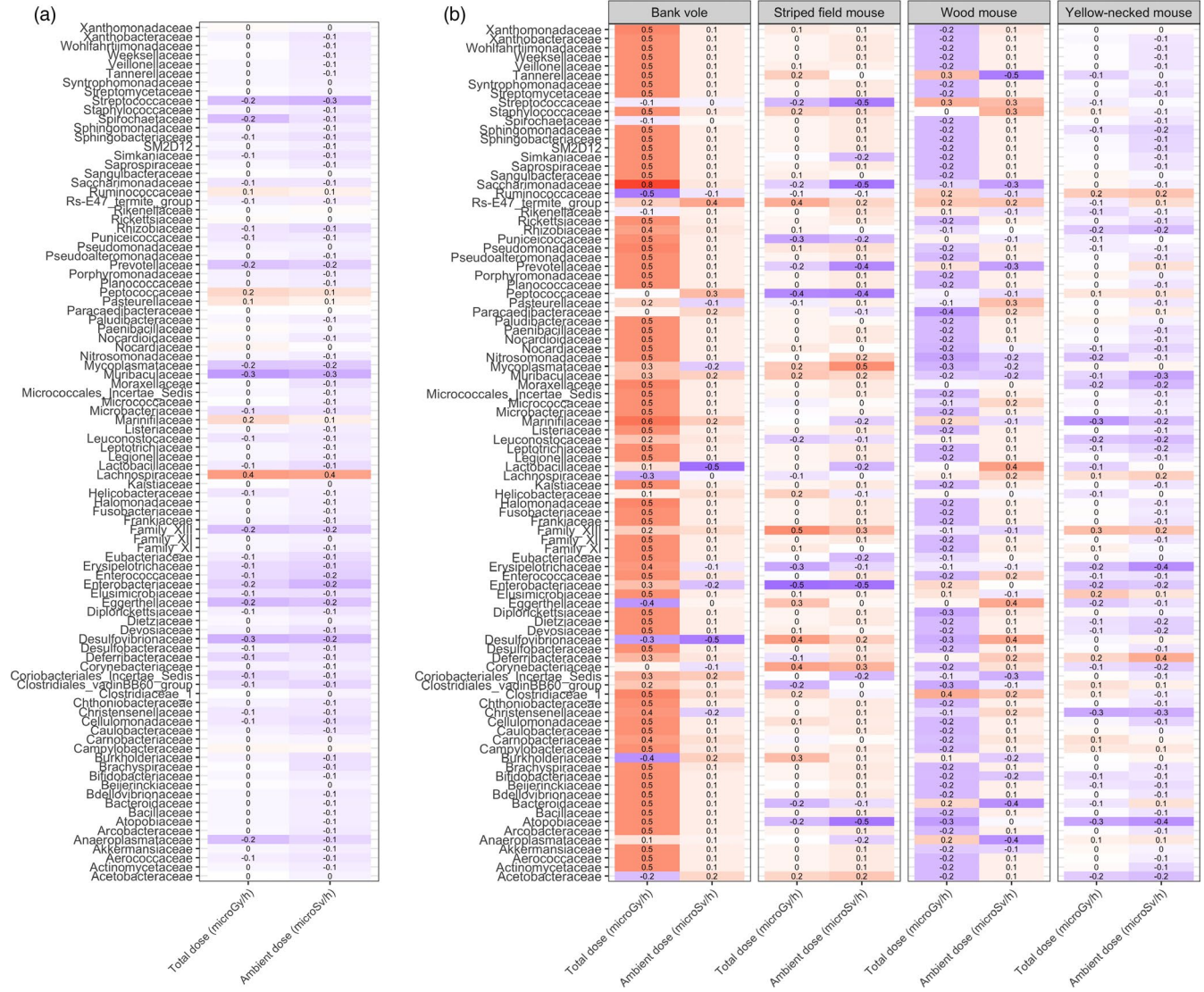


**FIGURE 3** Heat maps showing correlations between the two radiation dose rate measures (total and ambient) and (a) clr values of bacterial genera in the vole guts and (b) clr values of bacterial genera in faecal samples from four small mammal species

that faecal samples were collected in 2017 from the Red Forest and guts collected from different animals and sites over a wider area of the CEZ in 2018). Fungal and bacterial association patterns of faecal samples from the four small mammal species were also markedly different to one another (Figures 3b and 4b).

The association analysis identified one bacterial family in bank vole gut samples that positively correlated with total absorbed dose rate (Lachnospiraceae,  $p < 0.001$ ; Figure 3) and one that negatively correlated with total absorbed dose rate (Muribaculaceae,  $p < 0.001$ ; Figure 3). Lachnospiraceae also significantly correlated with ambient dose rate ( $p < 0.001$ ; Figure 3). The association analysis also identified one bacterial family from bank vole faeces that correlated with total absorbed dose rate (Saccharimonadaceae,  $p = 0.004$ ; Figure 3).

Two fungal families in bank vole gut samples were correlated with total absorbed dose rate, with Steccherinaceae negatively correlated ( $p = 0.006$ ) and Strophariaceae positively correlated ( $p = 0.006$ ; Figure 4). Steccherinaceae also correlated with ambient dose rate

( $p = 0.002$ ; Figure 4). There were no fungal families from faecal samples that were correlated with total or ambient dose rate (Figure 4).

### 3.6 | How do Firmicute: Bacteroidete ratios vary according to total absorbed dose rate category?

When using clr-transformed data, F:B was  $< 0$  in vole guts (Figure S12a). When using relative abundance data, voles in the 'high' total absorbed dose rate category had slightly higher F:B than those in the 'low' and 'medium' categories (Figure S12b). The Kruskal-Wallis model indicated no effect of total absorbed dose rate category on F:B in bank vole guts ( $X^2 = 5.556$ ,  $df = 2$ ,  $p = 0.062$ ). For the faecal sample data, only striped field mice and yellow-necked mice had data for animals in more than one absorbed dose rate category, that is, medium and high for both. The Kruskal-Wallis analysis was not significant for either striped field mice ( $X^2 = 0.012$ ,  $df = 1$ ,

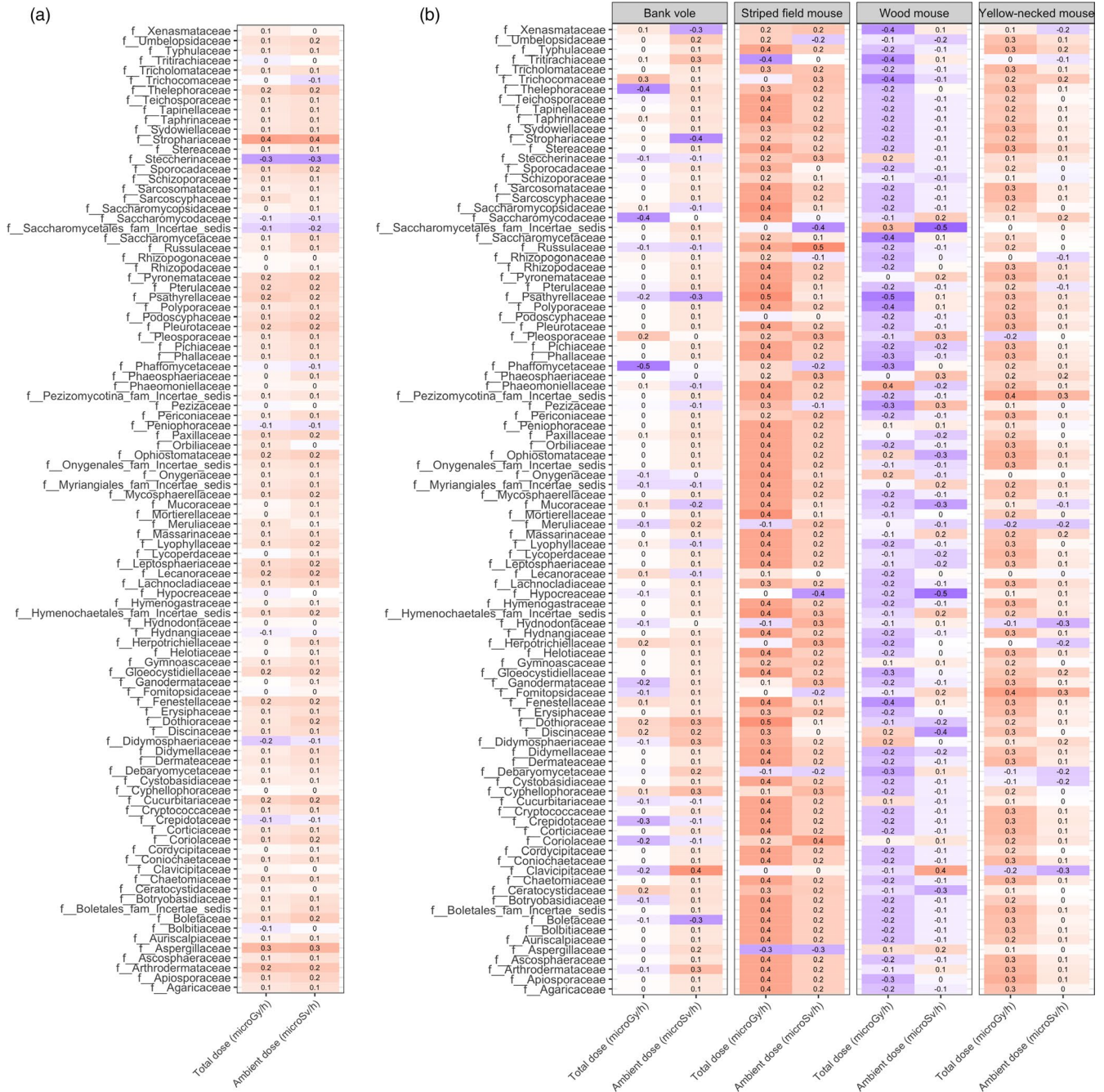


**FIGURE 4** Correlations between the two radiation dose measures (total absorbed and ambient dose rates) and (a) clr values of fungal genera in vole guts and (b) clr values of fungal genera in faecal samples from four small mammal species

$p = 0.911$ ) or yellow-necked mice ( $X^2 = 0.019$ ,  $df = 1$ ,  $p = 0.896$ ), meaning there were no differences in F:B between the 'medium' and 'high' categories for these two species (Figure S12c).

### 4 | DISCUSSION

In this study we present the first analyses of small mammal faecal and gut microbial communities from the CEZ for which individual total absorbed dose rates have been estimated. This study also

presents the first data from Chernobyl on the fungal component of the gut microbiome, and considers a wider range of small mammal species than previously studied, which have been limited to bank voles (Lavrinenko, Mappes, et al., 2018; Lavrinenko, Tukalenko, et al., 2018). Previous papers used faecal samples to characterise the small mammal gut microbiome (Lavrinenko, Mappes, et al., 2018; Lavrinenko, Tukalenko, et al., 2018), whereas our study also provides the first data on the true gut microbiome of Chernobyl bank voles using samples from the distal section of the caecum.

We provide novel evidence that radiation has limited effects on the microbial communities associated with the gut of a wild mammal species. Across all four host species, partial Mantel tests demonstrated that animals experiencing similar radiation exposure also had similar microbiome composition; this relationship was independent of sampling location. Although we identified detectable effects of radiation exposure category on both bacterial and fungal gut microbiome composition of bank voles, the effect sizes were limited, and the results were not robust once geographic distances were included in the analysis. Given that microbes are actually highly resistant to death when exposed to radiation (e.g. a high acute (>10 kGy) radiation dose is needed to eliminate fungi and bacteria from soils; (McNamara et al., 2003; Whicker & Schultz, 1982), environmental radiation exposure at sites such as Chernobyl is unlikely to affect the gut microbiome directly (but see discussion below about indirect drivers).

For bank voles, we observed differences in microbial communities associated with the gut and faeces, in agreement with previous studies of various host species (Ingala et al., 2018; Leite et al., 2019). We also observed significant differences in the relationships between radiation and gut/faecal microbial families. Consequently, faecal sampling may not give a good representation of gut communities nor of the effect of stressors on the gut microbiome. This may be because different taxa are being excreted to those that are retained in the gut, and animals may be shedding gut microbial communities in the faeces based on factors that relate indirectly to radiation exposure. For example, if radiation exposure causes changes in habitat quality, food availability or host physiology/metabolism/immunity, any of these could influence how the gut interacts with its microbiome, and subsequently what taxa are retained or shed (Friberg et al., 2019; Joyce et al., 2014; Newbold et al., 2019; Schirmer et al., 2016). Faecal communities are readily influenced by diet (Ingala et al., 2018; McKenney et al., 2018), suggesting radiation contamination and diet may be closely linked in the CEZ, though this may not necessarily imply a direct causal relationship between current radiation exposures and diet. The highly contaminated Red Forest area is of poor habitat quality, in part as a consequence of ecosystem damage following the Chernobyl accident in 1986, and most Red Forest sites in 2017 and 2018 were recovering from a recent wildfire event. Furthermore, bank vole gut samples were collected in 2018 from across the CEZ, whereas the faeces samples collected in 2017 were all from inside the Red Forest (including from a number of sites that had been recently burnt), which may also be influencing the observed differences between the gut and faecal samples. In addition, the host microbiome, including the fungal component, is influenced by the immune system (Enaud et al., 2018), which in turn is affected by radiation exposure (Jin et al., 2017), and so there is a clear route for radiation exposure to indirectly influence the host microbiome. However, given the vital role of the microbiome in host functioning, perhaps more important than compositional changes in the microbiome are the functional changes that radiation exposure confers. Further work with shotgun metagenomics or metatranscriptomics is required to determine

the effect of radiation exposure on microbiome function, and the implications of this for host fitness.

We found that sampling site is also a significant predictor of bacterial beta-diversity. Geographical location is known to affect bacterial community composition (Antwis et al., 2018; Griffiths et al., 2018), and here we also provide novel evidence that geography affects fungal community composition. Together our results suggest that any variation in microbiome composition arising from proximity to the Chernobyl Nuclear Power Plant is more likely a habitat effect than a result of radiation exposure. All animals in the 'high' total absorbed dose rates (>42  $\mu\text{Gy/hr}$ ) were collected from within the Red Forest. Other studies of radiation effects in CEZ wildlife, including the microbiome studies of Lavrinienko, Mappes, et al. (2018) and Lavrinienko, Tukalenko, et al. (2018), also have their most contaminated sampling sites within the Red Forest. The Red Forest is an area of poor habitat quality where soil and water conditions do not favour high biological diversity. The forest was also severely damaged in 1986 from the accident at the Chernobyl Nuclear Power Plant and has not fully recovered. Furthermore, some of our 2017 Red Forest sampling sites were showing signs of fire damage from a large fire in July 2016. Any study that uses the Red Forest as a location for radiation effect studies on wildlife needs to consider the historical impacts of radiation and other stressors (e.g. wildfires) on this area of the CEZ (Beresford, Horemans, et al., 2020).

The gut communities of bank voles showed similar changes in composition in response to both ambient and total dose radiation measures, although relationships were generally less strong for ambient dose compared with total dose. This may be due to differences in the way that individual dose rates are assigned; every individual from a site is assigned the same ambient dose rate, whereas total absorbed dose rate is calculated on an individual basis. We also identified a limited number of bacterial and fungal taxa with a significant association with total absorbed dose rate of the host animals in gut samples. These taxa may serve as useful biomarkers for radiation exposure in mammals, although more work is required to determine if these patterns are consistent across different host species and studies. Our data from faecal samples indicate that the relationship between the small mammal microbiomes and total absorbed dose rate of the host may vary from species to species, although there were relatively few detectable relationships between radiation dose and clr values for individual genera. However, Figures 3 and 4 indicate that faecal sample communities exhibited considerably different results for the two dose measures. Given the weak correlation between ambient and total absorbed dose rates and that the latter is the quantity most reflective of an animal's radiation exposure, ambient dose should not be used in radiation effects studies.

Firmicutes and Bacteroidetes are the most abundant phyla within the microbiome of small mammals; Firmicutes have been linked to processes such as the generation of metabolites, fat storage, angiogenesis and immune system maturation (Weldon et al., 2015). Lavrinienko, Mappes, et al. (2018) found a twofold

increase in F:B in bank vole faeces from areas of elevated radionuclide contamination in the CEZ (these sites would span our 'medium' and 'high' total absorbed dose rate categories) compared with areas of lower contamination in the CEZ and sites close to Kiev. The authors attribute a twofold increase in F:B to potential changes in diet arising from reduced arthropod densities in their higher contamination areas of the CEZ (referring to earlier work of Møller & Mousseau, 2009), the findings of which have been contested (Beresford, Scott, et al., 2020; Garnier-Laplace et al., 2013; Smith, 2020) and/or an active increase in the consumption of plant-based foods. Indeed, F:B in faeces has previously been used as a marker of changes in diet (Carmody et al., 2015). However, as Lavrinienko, Mappes, et al. (2018) acknowledge, bank vole diet is normally dominated by plant material, with only occasional consumption of invertebrates. Consequently, the effect of any reduction in arthropod consumption on the bank vole faecal microbiome F:B would likely be minimal. In the present study, we found no evidence of altered F:B in bank vole gut samples based on total absorbed radiation dose rate category suggesting similar bank vole diets across our study locations, including inside and outside the Red Forest.

To our knowledge, we present here the first demonstration that host species predicted faecal fungal community composition in ground-dwelling small mammal populations; fungal community compositions are an under-explored aspect of host-associated microbiomes in general (Antwis et al., 2020; Rowan-Nash et al., 2019). Host-associated fungal communities may be vital for a range of diverse functions including fat, carbon and nitrogen metabolism (Heisel et al., 2017; Wegley et al., 2007), degradation of dietary carbohydrates (Yang et al., 2018), resistance to infectious disease (Kearns et al., 2017), modulating host immune responses (Enaud et al., 2018; Yeung et al., 2020), and even behavioural traits such as host dispersal (Lu et al., 2010). We also show host species predicted bacterial community composition, which supports the results of previous studies on a range of host species (Davenport et al., 2017; Mazel et al., 2018; Youngblut et al., 2019), including small mammals (Knowles et al., 2019). We found no effect of sex on bacterial or fungal communities of the gut or faecal samples from any host species; previous studies have found mixed effects of sex on microbiome composition of small mammals (Knowles et al., 2019; Lavrinienko, Mappes, et al., 2018; Weldon et al., 2015).

## 5 | CONCLUSIONS

Here we show the gut communities of small mammal species are not directly affected by total radiation dose in the CEZ, but they are susceptible to differences in habitat type or quality. We found evidence that faecal communities are associated with radiation exposure independent of geographic location, but that these communities were not representative of true gut communities. In this study, we have identified two bacterial (Lachnospiraceae and Muribaculaceae) and

two fungal (Steccherinaceae and Strophariaceae) families in the guts of bank voles, which may serve as biomarkers of exposure to radiation. However, our findings would need verification in further studies considering a range of host species before these families could be recommended as robust biomarkers of small mammal radiation exposure.

In contrast to the findings of a published study of small mammal microbiomes in the CEZ (Lavrinienko, Mappes, et al., 2018; Lavrinienko, Tukalenko, et al., 2018), we did not see any effect of estimated radiation exposure on the F:B ratio (the earlier papers considered ambient dose rate only). Recognising the high variability in the individual-level radiation exposure measurements at some of our sites, our results provide evidence that total absorbed radiation dose should be used for radiation effects studies rather than site-level ambient dose rate measurements. Ambient dose rate was also not a reliable predictor of comparative total dose rates.

Given the importance of the microbiome to host health and the limited studies on microbiome (especially fungal microbiome and gut microbiome) in wild animals, further studies are required to understand whether different host species respond differently to radiation exposure in the CEZ, and the mechanisms of host physiology that regulate these. For this, it is important to establish directionality, that is, whether the host microbiome alters host physiology in response to radiation exposure or vice versa. Furthermore, changes in diet resulting from the impacts of radiation on the ecosystem (e.g. in an area such as the Red Forest), rather than the host, may also be expected to affect the gut microbiome. More work is required to understand the mechanisms that are driving changes in host microbiomes of wildlife in general, and the implications of this for host function and fitness.

## ACKNOWLEDGEMENTS

The work described in this paper was conducted within the TREE (<https://tree.ceh.ac.uk/>) and RED FIRE (<https://www.ceh.ac.uk/redfire>) projects. TREE was funded by the Natural Environment Research Council (NERC), Radioactive Waste Management Ltd. and the Environment Agency as part of the RATE Programme; RED FIRE was a NERC Urgency Grant. For the 2017 study, the GMS 310 core gamma logger was kindly loaned by John Caunt Scientific Ltd.

## CONFLICT OF INTEREST STATEMENT

REA is an associate editor for the Journal of Animal Ecology.

## AUTHORS' CONTRIBUTIONS

M.D.W., N.A.B. and S.G. designed the study and undertook sample collection (along with R.F., J.A.J., C.L.B., E.P. and L.W.); S.G. characterised the sites; N.A.B. and R.F. live-monitored small mammals; R.E.A. conducted the DNA extraction, molecular work and statistical analysis; R.E.A., N.A.B. and M.D.W. wrote the paper; all the authors revised and approved the final manuscript.

## DATA AVAILABILITY STATEMENT

Sequence data are available from the NCBI SRA database under project numbers PRJNA594002 and PRJNA592322.

## ORCID

Rachael E. Antwis  <https://orcid.org/0000-0002-8849-8194>

Nicholas A. Beresford  <https://orcid.org/0000-0002-8722-0238>

Joseph A. Jackson  <https://orcid.org/0000-0003-0330-5478>

Michael D. Wood  <https://orcid.org/0000-0002-0635-2387>

## REFERENCES

- Antwis, R. E., Cox, M., & Harrison, X. A. (2020). *Host microbiomes of soils, plants and animals: An integrated approach*. Cambridge University Press.
- Antwis, R. E., Lea, J. M. D., Unwin, B., & Shultz, S. (2018). Gut microbiome composition is associated with spatial structuring and social interactions in semi-feral Welsh Mountain ponies. *Microbiome*, 6(1), 207. <https://doi.org/10.1186/s40168-018-0593-2>
- Beaugelin-Seiller, K., Garnier-Laplace, J., & Beresford, N. A. (2020). Estimating radiological exposure of wildlife in the field. *Journal of Environmental Radioactivity*, 211. <https://doi.org/10.1016/j.jenvrad.2018.10.006>
- Beresford, N. A., Barnett, C. L., Gashchak, S., Kashparov, V., Kirieiev, S. I., Levchuk, S., Morozova, V., Smith, J. T., & Wood, M. D. (2021). Wildfires in the Chernobyl exclusion zone – Risks and consequences. *Integrated Environmental Assessment and Management*. <https://doi.org/10.1002/ieam.4424>
- Beresford, N. A., Barnett, C. L., Gashchak, S., Maksimenko, A., Guliachenko, E., Wood, M. D., & Izquierdo, M. (2020). Radionuclide transfer to wildlife at a 'Reference site' in the Chernobyl Exclusion Zone and resultant radiation exposures. *Journal of Environmental Radioactivity*, 211, 105661. <https://doi.org/10.1016/j.jenvrad.2018.02.007>
- Beresford, N. A., Gaschak, S., Barnett, C. L., Howard, B. J., Chizhevsky, I., Strømman, G., Oughton, D. H., Wright, S. M., Maksimenko, A., & Copplestone, D. (2008). Estimating the exposure of small mammals at three sites within the Chernobyl Exclusion Zone – A test application of the ERICA Tool. *Journal of Environmental Radioactivity*, 99(9), 1496–1502. <https://doi.org/10.1016/j.jenvrad.2008.03.002>
- Beresford, N. A., Gaschak, S., Maksimenko, A., & Wood, M. D. (2016). The transfer of <sup>137</sup>Cs, <sup>Pu</sup> isotopes and <sup>90</sup>Sr to bird, bat and ground-dwelling small mammal species within the Chernobyl Exclusion Zone. *Journal of Environmental Radioactivity*, 153, 231–236. <https://doi.org/10.1016/j.jenvrad.2015.12.027>
- Beresford, N. A., Horemans, N., Copplestone, D., Raines, K. E., Orizaola, G., Wood, M. D., Laanen, P., Whitehead, H. C., Burrows, J. E., Tinsley, M. C., Smith, J. T., Bonzom, J.-M., Gagnaire, B., Adam-Guillermin, C., Gashchak, S., Jha, A. N., de Menezes, A., Willey, N., & Spurgeon, D. (2020). Towards solving a scientific controversy – The effects of ionising radiation on the environment. *Journal of Environmental Radioactivity*, 211, 106033. <https://doi.org/10.1016/j.jenvrad.2005.01.004>
- Beresford, N. A., Scott, E. M., & Copplestone, D. (2020). Field effects studies in the Chernobyl Exclusion Zone: Lessons to be learnt. *Journal of Environmental Radioactivity*, 211. <https://doi.org/10.1016/j.jenvrad.2019.01.005>
- Brown, J. E., Alfonso, B., Avila, R., Beresford, N. A., Copplestone, D., & Hosseini, A. (2016). A new version of the ERICA tool to facilitate impact assessments of radioactivity on wild plants and animals. *Journal of Environmental Radioactivity*, 153, 141–148. <https://doi.org/10.1016/j.jenvrad.2015.12.011>
- Callahan, B. J., McMurdie, P. J., Rosen, M. J., Han, A. W., Johnson, A. J. A., & Holmes, S. P. (2016). DADA2: High-resolution sample inference from Illumina amplicon data. *Nature Methods*, 13(7), 581–583. <https://doi.org/10.1038/nmeth.3869>
- Caporaso, J. G., Lauber, C. L., Walters, W. A., Berg-lyons, D., Lozupone, C. A., Turnbaugh, P. J., Fierer, N., Knight, R. (2010). Global patterns of 16S rRNA diversity at a depth of millions of sequences per sample. <https://doi.org/10.1073/pnas.1000080107/-/DCSupplemental.www.pnas.org/cgi/doi/10.1073/pnas.1000080107>
- Carmody, R. N., Gerber, G. K., Luevano, J. M., Gatti, D. M., Somes, L., Svenson, K. L., & Turnbaugh, P. J. (2015). Diet dominates host genotype in shaping the murine gut microbiota. *Cell Host and Microbe*, 17(1), 72–84. <https://doi.org/10.1016/j.chom.2014.11.010>
- Copplestone, D., Bielby, S., Jones, S., Patton, D., Daniel, C., & Gize, I. (2001). *Impact assessment of ionising radiation on wildlife*. R&D Publication 128, Environment Agency and English Nature, Bristol.
- Currie, L. (1968). Limits for qualitative detection and quantitative determination. Application to radiochemistry. *Analytical Chemistry*, 40, 586–593. <https://doi.org/10.1021/ac60259a007>
- Czirják, G. Á., Møller, A. P., Mousseau, T. A., & Heeb, P. (2010). Microorganisms associated with feathers of barn swallows in radioactively contaminated areas around chernobyl. *Microbial Ecology*, 60(2), 373–380. <https://doi.org/10.1007/s00248-010-9716-4>
- Davenport, E. R., Sanders, J. G., Song, S. J., Amato, K. R., Clark, A. G., & Knight, R. (2017). The human microbiome in evolution. *BMC Biology*, 15(1), 1–12. <https://doi.org/10.1186/s12915-017-0454-7>
- Davis, N. M., Proctor, D. M., Holmes, S. P., Relman, D. A., & Callahan, B. J. (2017). Simple statistical identification and removal of contaminant sequences in marker-gene and metagenomics data. *BioRxiv*, 1–14. <https://doi.org/10.1101/221499>
- Demers, M., Dagnault, A., & Desjardins, J. (2014). A randomized double-blind controlled trial: Impact of probiotics on diarrhea in patients treated with pelvic radiation. *Clinical Nutrition*, 33(5), 761–767. <https://doi.org/10.1016/j.clnu.2013.10.015>
- Dinno, A. (2017). *dunn.test: Dunn's test of multiple comparisons using rank sums*. R package version 1.3.5. Retrieved from <https://CRAN.R-project.org/package=dunn.test>
- Dubois, A., & Walker, R. I. (1988). Gastrointestinal injury associated with the acute radiation syndrome. *Gastroenterology*, 95, 500–507.
- Enaud, R., Vandenberght, L.-E., Coron, N., Bazin, T., Prevel, R., Schaevebeke, T., Berger, P., Fayon, M., Lamireau, T., & Delhaes, L. (2018). The mycobioime: A neglected component in the microbiota-gut-brain axis. *Microorganisms*, 6(1), 22. <https://doi.org/10.3390/microorganisms6010022>
- Fawkes, R. (2018). *An innovative portable detector for the live-monitoring of radionuclides in small terrestrial animals*. Retrieved from [http://usir.salford.ac.uk/47893/1/ThesisRossFawkesv18.07.20\\_Final.pdf](http://usir.salford.ac.uk/47893/1/ThesisRossFawkesv18.07.20_Final.pdf)
- Friberg, I. M., Taylor, J. D., & Jackson, J. A. (2019). Diet in the driving seat: Natural diet-immunity-microbiome interactions in wild fish. *Frontiers in Immunology*, 10, 243. <https://doi.org/10.3389/fimmu.2019.00243>
- Garnier-Laplace, J., Geras'kin, S., Della-Vedova, C., Beaugelin-Seiller, K., Hinton, T. G., Real, A., & Oudalova, A. (2013). Are radiosensitivity data derived from natural field conditions consistent with data from controlled exposures? A case study of Chernobyl wildlife chronically exposed to low dose rates. *Journal of Environmental Radioactivity*, 121, 12–21. <https://doi.org/10.1016/j.jenvrad.2012.01.013>
- Gaschak, S. P., Maklyuk, Y. A., Maksimenko, A. M., Bondarkov, M. D., Jannik, G. T., & Farfán, E. B. (2011). Radiation ecology issues associated with murine rodents and shrews in the Chernobyl Exclusion Zone. *Health Physics*, 101(4), 416–430. <https://doi.org/10.1097/HP.0b013e31821e123f>
- Gloor, G. B., Macklaim, J. M., Pawlowsky-Glahn, V., & Egozcue, J. J. (2017). Microbiome datasets are compositional: And this is not optional. *Frontiers in Microbiology*, 8, 1–6. <https://doi.org/10.3389/fmicb.2017.02224>
- Goudarzi, M., Mak, T. D., Jacobs, J. P., Moon, B.-H., Strawn, S. J., Braun, J., Brenner, D. J., Fornace, A. J., & Li, H.-H. (2016). An integrated multi-omic approach to assess radiation injury on the host-microbiome axis. *Radiation Research*, 186(3), 219. <https://doi.org/10.1667/rr14306.1>

- Griffiths, S. M., Galambao, M., Rowntree, J., Goodhead, I., Hall, J., O'Brien, D., Atkinson, N., & Antwis, R. E. (2019). Complex associations between cross-kingdom microbial endophytes and host genotype in ash dieback disease dynamics. *Journal of Ecology*, 1–19. <https://doi.org/10.1111/1365-2745.13302>
- Griffiths, S. M., Harrison, X. A., Weldon, C., Wood, M. D., Pretorius, A., Hopkins, K., Fox, G., Preziosi, R. F., & Antwis, R. E. (2018). Genetic variability and ontogeny predict microbiome structure in a disease-challenged montane amphibian. *The ISME Journal*, 12, 2506–2517. <https://doi.org/10.1038/s41396-018-0167-0>
- Heisel, T., Montassier, E., Johnson, A., Al-Ghalith, G., Lin, Y.-W., Wei, L.-N., Knights, D., & Gale, C. A. (2017). High-fat diet changes fungal microbiomes and interkingdom relationships in the murine gut. *mSphere*, 2(5), 1–14. <https://doi.org/10.1128/msphere.00351-17>
- ICRP. (2008). *Environmental protection: The concept and use of reference animals and plants*, ICRP publication 108, Ann. ICRP 38, 4–6, 2008.
- Ingala, M. R., Simmons, N. B., Wultsch, C., Krampis, K., Speer, K. A., & Perkins, S. L. (2018). Comparing microbiome sampling methods in a wild mammal: Fecal and intestinal samples record different signals of host ecology, evolution. *Frontiers in Microbiology*, 9, 1–13. <https://doi.org/10.3389/fmicb.2018.00803>
- Jin, C., Zeng, Z., Fu, Z., & Jin, Y. (2016). Oral imazalil exposure induces gut microbiota dysbiosis and colonic inflammation in mice. *Chemosphere*, 349–358. <https://doi.org/10.1016/j.chemosphere.2016.06.105>
- Jin, Y., Wu, S., Zeng, Z., & Fu, Z. (2017). Effects of environmental pollutants on gut microbiota. *Environmental Pollution*, 222, 1–9. <https://doi.org/10.1016/j.envpol.2016.11.045>
- Jin, Y., Zeng, Z., Wu, Y., Zhang, S., & Fu, Z. (2015). Oral exposure of mice to carbendazim induces hepatic lipid metabolism disorder and gut microbiota dysbiosis. *Toxicological Sciences*, 147(1), 116–126. <https://doi.org/10.1093/toxsci/kfv115>
- Joly Condette, C., Bach, V., Mayeur, C., Gay-Quéheillard, J., & Khorsi-Cauet, H. (2015). Chlorpyrifos exposure during perinatal period affects intestinal microbiota associated with delay of maturation of digestive tract in rats. *Journal of Pediatric Gastroenterology and Nutrition*, 61(1), 30–40. <https://doi.org/10.1097/MPG.00000000000000734>
- Joyce, S. A., MacSharry, J., Casey, P. G., Kinsella, M., Murphy, E. F., Shanahan, F., Hill, C., & Gahan, C. G. M. (2014). Regulation of host weight gain and lipid metabolism by bacterial bile acid modification in the gut. *Proceedings of the National Academy of Sciences of the United States of America*, 111(20), 7421–7426. <https://doi.org/10.1073/pnas.1323599111>
- Kan, H., Zhao, F., Zhang, X. X., Ren, H., & Gao, S. (2015). Correlations of gut microbial community shift with hepatic damage and growth inhibition of *carassius auratus* induced by pentachlorophenol exposure. *Environmental Science and Technology*, 49(19), 11894–11902. <https://doi.org/10.1021/acs.est.5b02990>
- Kearns, P. J., Fischer, S., Fernández-Beascoetxea, S., Gabor, C. R., Bosch, J., Bowen, J. L., Tlustý, M. F., & Woodhams, D. C. (2017). Fight fungi with fungi: Antifungal properties of the amphibian microbiome. *Frontiers in Microbiology*, 8, 1–12. <https://doi.org/10.3389/fmicb.2017.02494>
- Knowles, S. C. L., Eccles, R. M., & Baltrūnaitė, L. (2019). Species identity dominates over environment in shaping the microbiota of small mammals. *Ecology Letters*, 22(5), 826–837. <https://doi.org/10.1111/ele.13240>
- Kozich, J. J., Westcott, S. L., Baxter, N. T., Highlander, S. K., & Schloss, P. D. (2013). Development of a dual-index sequencing strategy and curation pipeline for analyzing amplicon sequence data on the MiSeq Illumina sequencing platform. *Applied and Environmental Microbiology*, 79(17), 5112–5120. <https://doi.org/10.1128/AEM.01043-13>
- Lahti, L., & Shetty, S. (2017). Tools for microbiome analysis in R. Microbiome package version 1.1.10013.
- Lavrinenko, A., Mappes, T., Tukalenko, E., Mousseau, T. A., Møller, A. P., Knight, R., Morton, J. T., Thompson, L. R., & Watts, P. C. (2018). Environmental radiation alters the gut microbiome of the bank vole *Myodes glareolus*. *ISME Journal*, 12(11), 2801–2806. <https://doi.org/10.1038/s41396-018-0214-x>
- Lavrinenko, A., Tukalenko, E., Mappes, T., & Watts, P. C. (2018). Skin and gut microbiomes of a wild mammal respond to different environmental cues. *Microbiome*, 6(1), 1–16. <https://doi.org/10.1186/s40168-018-0595-0>
- Leite, G., Weitsman, S., Celly, S., Morales, W., Sedighi, R., Mathur, R., Parodi, G., Villanueva-Millan, M. J., Rezaie, A., Sanchez, M., Enjily, A., Chua, K. S., Singer-Englar, T., Chang, C., & Pimentel, M. (2019). Sa1911 – Analysis of the small intestinal microbiome reveals marked differences from stool microbiome in a large scale human cohort: Redefining the 'gut microbiome'. *Gastroenterology*, 156(6), S-449–S-450. [https://doi.org/10.1016/s0016-5085\(19\)37977-6](https://doi.org/10.1016/s0016-5085(19)37977-6)
- Liu, M.-M., Li, S.-T., Shu, Y., & Zhan, H.-Q. (2017). Probiotics for prevention of radiation-induced diarrhea: A meta-analysis of randomized controlled trials. *PLoS ONE*, 12(6), e0178870. <https://doi.org/10.1371/journal.pone.0178870>
- Lu, K., Abo, R. P., Schlieper, K. A., Graffam, M. E., Levine, S., Wishnok, J. S., Swenberg, J. A., Tannenbaum, S. R., & Fox, J. G. (2014). Arsenic exposure perturbs the gut microbiome and its metabolic profile in mice: An integrated metagenomics and metabolomics analysis. *Environmental Health Perspectives*, 122(3), 284–291. <https://doi.org/10.1289/ehp.1307429>
- Lu, M., Wingfield, M. J., Gillette, N. E., Mori, S. R., & Sun, J. H. (2010). Complex interactions among host pines and fungi vectored by an invasive bark beetle. *New Phytologist*, 187(3), 859–866. <https://doi.org/10.1111/j.1469-8137.2010.03316.x>
- Martin, M. (2011). Cutadapt removes adapter sequences from high-throughput sequencing reads. *EMBnet journal*, 17, 10–12.
- Maurice, C. F., Cl Knowles, S., Ladau, J., Pollard, K. S., Fenton, A., Pedersen, A. B., & Turnbaugh, P. J. (2015). Marked seasonal variation in the wild mouse gut microbiota. *ISME Journal*, 9(11), 2423–2434. <https://doi.org/10.1038/ismej.2015.53>
- Mazel, F., Davis, K. M., Loudon, A., Kwong, W. K., Groussin, M., & Parfrey, L. W. (2018). Is host filtering the main driver of phyllosymbiosis across the tree of life? *MSystems*, 3(5), 1–15. <https://doi.org/10.1128/msyst.00097-18>
- McFall-Ngai, M., Hadfield, M. G., Bosch, T. C. G., Carey, H. V., Domazet-Lošo, T., Douglas, A. E., Dubilier, N., Eberl, G., Fukami, T., Gilbert, S. F., Hentschel, U., King, N., Kjelleberg, S., Knoll, A. H., Kremer, N., Mazmanian, S. K., Metcalf, J. L., Neelson, K., Pierce, N. E., ... Wernegreen, J. J. (2013). Animals in a bacterial world, a new imperative for the life sciences. *Proceedings of the National Academy of Sciences of the United States of America*, 110(9), 3229–3236. <https://doi.org/10.1073/pnas.1218525110>
- McKenney, E. A., Koelle, K., Dunn, R. R., & Yoder, A. D. (2018). The ecosystem services of animal microbiomes. *Molecular Ecology*, 0–1. <https://doi.org/10.1111/mec.14532>
- McKenney, E. A., O'Connell, T. M., Rodrigo, A., & Yoder, A. D. (2018). Feeding strategy shapes gut metagenomic enrichment and functional specialization in captive lemurs. *Gut Microbes*, 9(3), 202–217. <https://doi.org/10.1080/19490976.2017.1408762>
- McKenney, E. A., Rodrigo, A., & Yoder, A. D. (2015). Patterns of gut bacterial colonization in three primate species. *PLoS ONE*, 10(5), 1–18. <https://doi.org/10.1371/journal.pone.0124618>
- McMurdie, P. J., & Holmes, S. (2013). Phyloseq: An R package for reproducible interactive analysis and graphics of microbiome census data. *PLoS ONE*, 8(4), e61217. <https://doi.org/10.1371/journal.pone.0061217>
- McNamara, N. P., Black, H. I. J., Beresford, N. A., & Parekh, N. R. (2003). Effects of acute gamma irradiation on chemical, physical and biological properties of soils. *Applied Soil Ecology*, 24(2), 117–132. [https://doi.org/10.1016/S0929-1393\(03\)00073-8](https://doi.org/10.1016/S0929-1393(03)00073-8)

- Meyer, D., & Buchta, C. (2019). *proxy: Distance and similarity measures*. R package version 0.4-23. Retrieved from <https://CRAN.R-project.org/package=proxy>
- Møller, A. P., & Mousseau, T. A. (2009). Reduced abundance of insects and spiders linked to radiation at Chernobyl 20 years after the accident. *Biology Letters*, 5(3), 356–359. <https://doi.org/10.1098/rsbl.2008.0778>
- Mousseau, T. A., & Moller, A. P. (2011). Landscape portrait: A look at the impacts of radioactive contaminants on Chernobyl's wildlife. *Bulletin of the Atomic Scientists*, 67(2), 38–46. <https://doi.org/10.1177/00963402111399747>
- Nasuti, C., Coman, M. M., Olek, R. A., Fiorini, D., Verdenelli, M. C., Cecchini, C., Silvi, S., Fedeli, D., & Gabbianelli, R. (2016). Changes on fecal microbiota in rats exposed to permethrin during postnatal development. *Environmental Science and Pollution Research*, 23(11), 10930–10937. <https://doi.org/10.1007/s11356-016-6297-x>
- Newbold, L. K., Robinson, A., Rasnaca, I., Lahive, E., Soon, G. H., Lapied, E., Oughton, D., Gashchak, S., Beresford, N. A., & Spurgeon, D. J. (2019). Genetic, epigenetic and microbiome characterisation of an earthworm species (*Octolasion lacteum*) along a radiation exposure gradient at Chernobyl. *Environmental Pollution*, 255, 113238. <https://doi.org/10.1016/j.envpol.2019.113238>
- Nguyen, N. H., Smith, D., Peay, K., & Kennedy, P. (2015). Parsing ecological signal from noise in next generation amplicon sequencing. *New Phytologist*, 205(4), 1389–1393. <https://doi.org/10.1111/nph.12923>
- Ogle, D. H., Wheeler, P., & Dinno, A. (2019). *FSA: Fisheries stock analysis*. R package version 0.8.25. Retrieved from <https://github.com/droglenc/FSA>
- Oksanen, J., Blanchet, B., Friendly, M., Kindt, R., Legendre, P., McGlenn, D., Minchin, P. R., O'Hara, R. B., Simpson, G. L., Solymos, P., Stevens, M. H. H., Szoecs, E., & Wagner, H. (2018). *vegan: Community ecology package*.
- Packey, C. D., & Ciorba, M. A. (2011). Microbial influences on the small intestinal response to radiation injury. *Current Opinion in Gastroenterology*, 46(4), 564–574. <https://doi.org/10.1016/j.cortex.2009.08.003>
- Quast, C., Pruesse, E., Yilmaz, P., Gerken, J., Schweer, T., Yarza, P., Peplies, J., & Glöckner, F. O. (2013). The SILVA ribosomal RNA gene database project: Improved data processing and web-based tools. *Nucleic Acids Research*, 41(D1), 590–596. <https://doi.org/10.1093/nar/gks1219>
- R Core Team. (2017). *R: A language and environment for statistical computing*. R Foundation for Statistical Computing.
- Rowan-Nash, A. D., Korry, B. J., Mylonakis, E., & Belenky, P. (2019). Cross-domain and viral interactions in the microbiome. *Microbiology and Molecular Biology Reviews*, 83(1), 1–63. <https://doi.org/10.1128/mubr.00044-18>
- RStudio Team. (2016). *RStudio: Integrated development for R*.
- Ruiz-González, M. X., Cziráj, G. Á., Genevoux, P., Møller, A. P., Mousseau, T. A., & Heeb, P. (2016). Resistance of feather-associated bacteria to intermediate levels of ionizing radiation near chernobyl. *Scientific Reports*, 6, 1–7. <https://doi.org/10.1038/srep22969>
- Schirmer, M., Smeekens, S. P., Vlamakis, H., Jaeger, M., Oosting, M., Franzosa, E. A., ter Horst, R., Jansen, T., Jacobs, L., Bonder, M. J., Kurilshikov, A., Fu, J., Joosten, L. A. B., Zhernakova, A., Huttenhower, C., Wijmenga, C., Netea, M. G., & Xavier, R. J. (2016). Linking the human gut microbiome to inflammatory cytokine production capacity. *Cell*, 167(4), 1125–1136.e8. <https://doi.org/10.1016/j.cell.2016.10.020>
- Schoch, C. L., Seifert, K. A., Huhndorf, S., Robert, V., Spouge, J. L., Levesque, C. A., Chen, W., Bolchacova, E., Voigt, K., Crous, P. W., Miller, A. N., Wingfield, M. J., Aime, M. C., An, K.-D., Bai, F.-Y., Barreto, R. W., Begerow, D., Bergeron, M.-J., Blackwell, M., ... Schindel, D. (2012). Nuclear ribosomal internal transcribed spacer (ITS) region as a universal DNA barcode marker for Fungi. *Proceedings of the National Academy of Sciences of the United States of America*, 109(16), 6241–6246. <https://doi.org/10.1073/pnas.1117018109>
- Shestopalov, V. (1996). *Atlas of Chernobyl Exclusion Zone*. Ukrainian Academy of Science.
- Smith, D. P., & Peay, K. G. (2014). Sequence depth, Not PCR replication, improves ecological inference from next generation DNA sequencing. *PLoS ONE*, 9(2), e90234. <https://doi.org/10.1371/journal.pone.0090234>
- Smith, J. (2020). Field evidence of significant effects of radiation on wildlife at chronic low dose rates is weak and often misleading. A comment on 'Is non-human species radiosensitivity in the lab a good indicator of that in the field? Making the comparison more robust'. *Journal of Environmental Radioactivity*, 211, 105895. <https://doi.org/10.1016/j.jenvrad.2019.01.007>
- Ulanovsky, A., Pröhl, G., & Gómez-Ros, J. M. (2008). Methods for calculating dose conversion coefficients for terrestrial and aquatic biota. *Journal of Environmental Radioactivity*, 99(9), 1440–1448. <https://doi.org/10.1016/j.jenvrad.2008.01.010>
- UNITE. (2017). *UNITE general FASTA release*. Version 01.12.2017.
- Viney, M. (2019). The gut microbiota of wild rodents: Challenges and opportunities. *Laboratory Animals*, 53(3), 252–258. <https://doi.org/10.1177/0023677218787538>
- Vives i Batlle, J., Balonov, M., Beaugelin-Seiller, K., Beresford, N. A., Brown, J., Cheng, J.-J., Copplesstone, D., Doi, M., Filistovic, V., Golikov, V., Horyna, J., Hosseini, A., Howard, B. J., Jones, S. R., Kamboj, S., Kryshev, A., Nedveckaite, T., Olyslaegers, G., Pröhl, G., ... Yu, C. (2007). Inter-comparison of absorbed dose rates for non-human biota. *Radiation and Environmental Biophysics*, 46(4), 349–373. <https://doi.org/10.1007/s00411-007-0124-1>
- Wegley, L., Edwards, R., Rodriguez-Brito, B., Liu, H., & Rohwer, F. (2007). Metagenomic analysis of the microbial community associated with the coral *Porites astreoides*. *Environmental Microbiology*, 9(11), 2707–2719. <https://doi.org/10.1111/j.1462-2920.2007.01383.x>
- Weldon, L., Abolins, S., Lenzi, L., Bourne, C., Riley, E. M., & Viney, M. (2015). The gut microbiota of wild mice. *PLoS ONE*, 10(8), 1–15. <https://doi.org/10.1371/journal.pone.0134643>
- Whicker, F. W., & Schultz, V. (1982). *Radioecology: Nuclear energy and the environment* (Vol. 2). CRC Press.
- Wickham, H. (2009). *ggplot2: Elegant graphics for data analysis*. Springer-Verlag.
- Williams, K., Milner, J., Boudreau, M. D., Gokulan, K., Cerniglia, C. E., & Khare, S. (2015). Effects of subchronic exposure of silver nanoparticles on intestinal microbiota and gut-associated immune responses in the ileum of Sprague-Dawley rats. *Nanotoxicology*, 9, 279–289. <https://doi.org/10.3109/17435390.2014.921346>
- Wu, J., Wen, X. W., Faulk, C., Boehnke, K., Zhang, H., Dolinoy, D. C., & Xi, C. (2016). Perinatal lead exposure alters gut microbiota composition and results in sex-specific bodyweight increases in adult mice. *Toxicological Sciences*, 151(2), 324–333. <https://doi.org/10.1093/toxsci/kfw046>
- Yang, S., Gao, X., Meng, J., Zhang, A., Zhou, Y., Long, M., Li, B., Deng, W., Jin, L., Zhao, S., Wu, D., He, Y., Li, C., Liu, S., Huang, Y., Zhang, H., & Zou, L. (2018). Metagenomic analysis of bacteria, fungi, bacteriophages, and helminths in the gut of giant pandas. *Frontiers in Microbiology*, 9, 1–16. <https://doi.org/10.3389/fmicb.2018.01717>
- Yeung, F., Chen, Y.-H., Lin, J.-D., Leung, J. M., McCauley, C., Devlin, J. C., Hansen, C., Cronkite, A., Stephens, Z., Drake-Dunn, C., Fulmer, Y. I., Shopsin, B. O., Ruggles, K. V., Round, J. L., Loke, P'ng, Graham, A. L., & Cadwell, K. (2020). Altered immunity of laboratory mice in the natural environment is associated with fungal colonization. *Cell Host and Microbe*, 1–14. <https://doi.org/10.1016/j.chom.2020.02.015>
- Yilmaz, P., Parfrey, L. W., Yarza, P., Gerken, J., Pruesse, E., Quast, C., Schweer, T., Peplies, J., Ludwig, W., & Glöckner, F. O. (2014). The SILVA and 'all-species Living Tree Project (LTP)' taxonomic

- frameworks. *Nucleic Acids Research*, 42(D1), 643–648. <https://doi.org/10.1093/nar/gkt1209>
- Youngblut, N. D., Reischer, G. H., Walters, W., Schuster, N., Walzer, C., Stalder, G., Ley, R. E., & Farnleitner, A. H. (2019). Host diet and evolutionary history explain different aspects of gut microbiome diversity among vertebrate clades. *Nature Communications*, 10(1), 1–15. <https://doi.org/10.1038/s41467-019-10191-3>
- Zhang, A., & Steen, T. Y. (2018). Gut microbiomics – A solution to unloose the Gordian knot of biological effects of ionizing radiation. *Journal of Heredity*, 109(2), 212–221. <https://doi.org/10.1093/jhered/esx059>
- Zhang, L., Rimal, B., Nichols, R. G., Tian, Y., Smith, P. B., Hatzakis, E., Chang, S.-C., Butenhoff, J. L., Peters, J. M., & Patterson, A. D. (2020). Perfluorooctane sulfonate alters gut microbiota-host metabolic homeostasis in mice. *Toxicology*, 431, 152365. <https://doi.org/10.1016/j.tox.2020.152365>
- Zhang, S., Jin, Y., Zeng, Z., Liu, Z., & Fu, Z. (2015). Subchronic exposure of mice to cadmium perturbs their hepatic energy metabolism and gut microbiome. *Chemical Research in Toxicology*, 28(10), 2000–2009. <https://doi.org/10.1021/acs.chemrestox.5b00237>

#### SUPPORTING INFORMATION

Additional supporting information may be found online in the Supporting Information section.

**How to cite this article:** Antwis RE, Beresford NA, Jackson JA, et al. Impacts of radiation exposure on the bacterial and fungal microbiome of small mammals in the Chernobyl Exclusion Zone. *J Anim Ecol*. 2021;90:2172–2187. <https://doi.org/10.1111/1365-2656.13507>